Current Biology, Volume *27*

Supplemental Information

The CDK8 Complex and Proneural Proteins Together Drive Neurogenesis from a Mesodermal Lineage

Shuo Luo and H. Robert Horvitz

Supplemental Figures and Legends

A

Genotype[a]	% I4-to-muscle transformation	*n*
hlh-3(n5564)	26	100
hlh-3; Ex[hlh-3(+)]_1	1	100
hlh-3; Ex[hlh-3(+)]_2	0	100
hlh-3; Ex[hlh-3(+)]_3	2	70
let-19(n5470)	19	300
let-19; Ex[let-19(+)]_1	3	100
let-19; Ex[let-19(+)]_2	0	100
let-19; Ex[let-19(+)]_3	4	100
hlh-3(n5469)	18	100
hlh-3; dpy-22(n5572)	62.5	200
hlh-3; dpy-22; Ex[dpy-22(+)]_1	20	50
hlh-3; dpy-22; Ex[dpy-22(+)]_2	19.7	66
hlh-3; dpy-22; Ex[dpy-22(+)]_3	17.5	40

a: Contain *oxIs322[Pmyo-2::mCh::H2B]* and *nIs310[Pnlp-13::gfp]*.

B

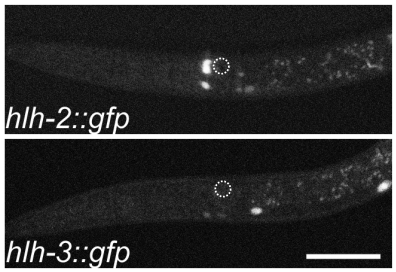

C

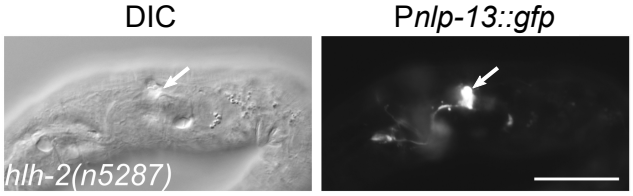

Figure S1. HLH proneural transcription factors and Mediator subunits promote I4 neurogenesis, and HLH proteins likely function in early embryogenesis. Related to Figures 1 and 2. (A) Extrachromosomal array containing *hlh-3*, *let-19* or *dpy-22* genomic sequence rescues I4 misspecification phenotype of *hlh-3*, *let-19* or *dpy-22* mutants, respectively. (B) Z-projection of the confocal images of L1 transgenic animals expressing either HLH-3::GFP or HLH-2::GFP fusion protein. The position of I4 is marked by the circle. No HLH-3 or HLH-2 expression is observed in the I4 neuron in newly hatched animals, suggesting that HLH proteins function in early embryogenesis to promote I4 development. (C) An arrested homozygous *hlh-2* mutant embryo expresses I4 GFP normally (arrows), suggesting a possible maternal contribution of HLH-2 to normal I4 neuronal cell-fate specification. Scale bar, 20 μm.

A

Neurotransmitter	Reporter gene	No. neurons expressing the reporter
Acetylcholine(Ach)	*unc-17*	~120
Glutamate(Glu)	*eat-4*	78
GABA	*unc-25, unc-47*	26
Serotonin(5HT)	*tph-1*	6
Dopamine(DA)	*cat-2*	8
Tyramine(TA)/Octopamine(OA)	*tdc-1*	4

B

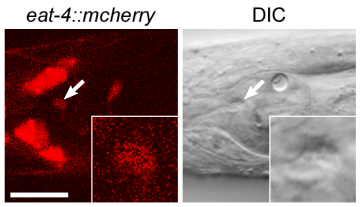

C

MS-derived neurons	Neurotransmitter	Reporter transgene	Neurogenesis
I3	Unknown	N/A	+
I4	Glutamate[a]	*eat-4::mCherry*	-
I6	Glutamate[a]	*eat-4::mCherry*	+
M1	Acetylcholine	P*unc-17::gfp*	+
M4	Acetylcholine	P*unc-17::gfp*	+
M5	Glutamate	*eat-4::mCherry*	+

a: Reporter transgene expression variable. See legend.

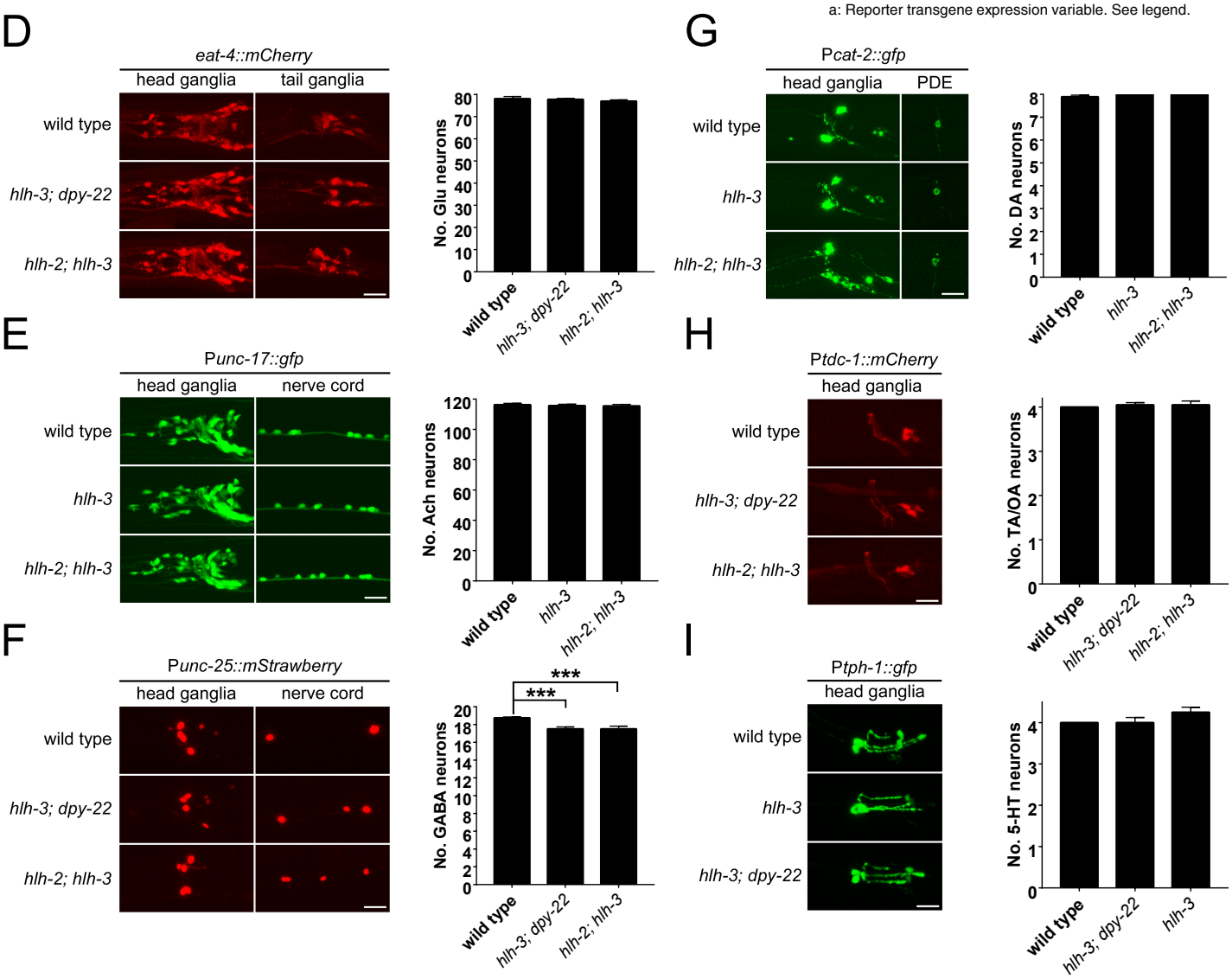

Figure S2. HLH-3 is mostly dispensable for neurogenesis. Related to Figure 2. (A) List of the neurotransmitter reporter transgenes used to examine neurogenesis in *hlh-3* mutants. (B) The I4 neuron expresses a reporter transgene for the glutamate transporter EAT-4 and might be glutamatergic (arrows and insets). (C) The other five MS-derived neurons are generated normally in *hlh-3(n5469)* mutant animals (n=40). The glutamatergic reporter transgene $P_{eat\text{-}4}$*::eat-4::mCherry* is expressed in I4 and I6 in only 10% (for I4) and 60% (for I6) of the wild-type animals examined. (D-I) HLH-3 and Mediator specifically promote I4 neurogenesis and are likely dispensable for most ectodermal neurogenesis. The generation of (D) glutamatergic (wild type: 78.1 ± 1.0, n=10; *hlh-2; hlh-3*: 77.0 ± 0.6, n=16; *hlh-3; dpy-22*: 77.8 ± 0.4, n=15), (E) cholinergic (wild type: 116.3 ± 0.9, n=13; *hlh-2; hlh-3*: 115.5 ± 1.0, n=15; *hlh-3; dpy-22*: 115.7 ± 0.9, n=17), (G) dopaminergic (wild type: 7.9 ± 0.1, n=19; *hlh-3*: 8.0 ± 0, n=20; *hlh-2; hlh-3*: 8.0 ± 0, n=19), (H) tyraminergic/octopaminergic (wild type: 4.0 ± 0, n=20; *hlh-2; hlh-3*: 4.0 ± 0.1, n=20; *hlh-3; dpy-22*: 4.0 ± 0.1, n=20), and (I) serotonergic (wild type: 4.0 ± 0, n=20; *hlh-3; dpy-22*: 4.0 ± 0.1, n=20; *hlh-3*: 4.2 ± 0.1, n=20) neurons is normal in *hlh-3* single and double mutants. The generation of (F) GABAergic (wild type: 18.8 ± 0.1, n=25; *hlh-2; hlh-3*: 17.5 ± 0.3, n=25; *hlh-3; dpy-22*: 17.5 ± 0.2, n=25, P<0.001) neurons in *hlh-3* double mutants is mildly reduced. We were unable to examine cholinergic neurons in *hlh-3; dpy-22* double mutants, because the cholinergic reporter transgene is tightly linked to *dpy-22*. In (I) we did not score the serotonergic HSN neurons, which are generated but fail to differentiate normally in *hlh-3* mutants and do not express the $P_{tph\text{-}1}$*::gfp* reporter transgene [S1]. The slightly higher numbers of serotonergic neurons in *hlh-3* mutants result from partial defects in the cell deaths of the sister cells of the serotonergic NSM neurons [S2] (I). All data represent mean ± s.e.m. ***, P<0.001 by student's t-test. Scale bars, 20 μm.

A

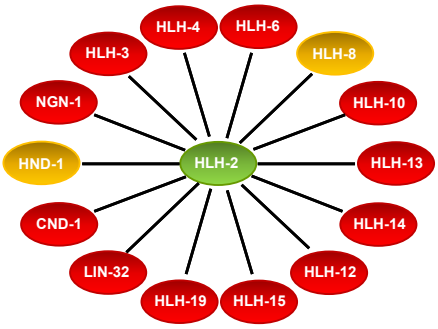

B

Genotype	% I4-to-muscle transformation	*n*
wild type[a]	0	100
cnd-1(gk781)[a]	0	200
cnd-1(gk718)[a]	0	200
ngn-1(ok2200)[a]	0	200
hlh-2(bx115); cnd-1(gk718)[b]	0	100
hlh-2(bx115); ngn-1(ok2200)[b]	0	200

a: Contains *oxIs322[*P*myo-2::mCherry::h2b]* and *nIs310[*P*nlp-13::gfp]*
b: Contains *nIs310[*P*nlp-13::gfp]*

C

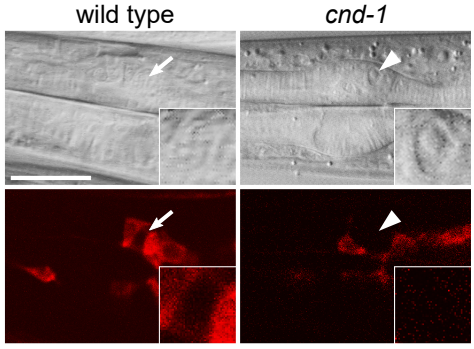

cnd-1(gk781)

Neuron (%)	I3	I4	I6	M1	M4	M5
wild type	75	100	100	98	100	85
missing	25	0	0	0	0	0
mislocalization	0	0	0	2	0	15

Contains *otIs173[*P*rgef-1::dsRed]*, *n*=65

D

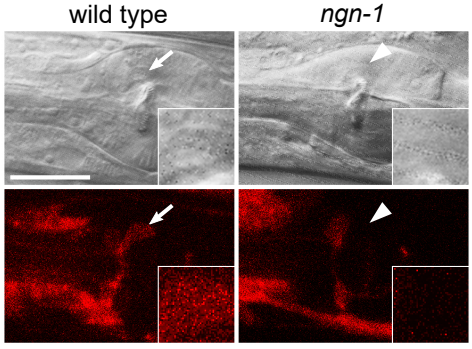

ngn-1(ok2200)

Neuron (%)	I3	I4	I6	M1	M4	M5
wild type	100	78	96	49	100	98
missing	0	0	0	41	0	0
mislocalization	0	22	4	10	0	2

Contains *otIs173[*P*rgef-1::dsRed]*, *n*=51

E

lin-32(e1926)

Neuron (%)	I3	I4	I6	M1	M4	M5
wild type	100	100	100	100	100	98
missing	0	0	0	0	0	0
mislocalization	0	0	0	0	0	2

Contains *otIs173[*P*rgef-1::dsRed]*, *n*=65

F

hlh-4(tm604)

Neuron (%)	I3	I4	I6	M1	M4	M5
wild type	100	100	96	100	100	96
missing	0	0	0	0	0	0
mislocalization	0	0	4	0	0	4

n=51

G

hlh-6(tm299)

Neuron (%)	I3	I4	I6	M1	M4	M5
wild type	100	100	100	100	100	100
missing	0	0	0	0	0	0
mislocalization	0	0	0	0	0	0

Contains *otIs173[*P*rgef-1::dsRed]*, *n*=50

H

hlh-10(ok516)

Neuron (%)	I3	I4	I6	M1	M4	M5
wild type	100	100	100	100	100	100
missing	0	0	0	0	0	0
mislocalization	0	0	0	0	0	0

Contains *otIs173[*P*rgef-1::dsRed]*, *n*=51

I

hlh-12(ok1532)

Neuron (%)	I3	I4	I6	M1	M4	M5
wild type	100	100	100	100	100	97
missing	0	0	0	0	0	0
mislocalization	0	0	0	0	0	3

Contains *otIs173[*P*rgef-1::dsRed]*, *n*=60

J

hlh-13(tm2279)

Neuron (%)	I3	I4	I6	M1	M4	M5
wild type	100	98	98	100	100	98
missing	0	0	0	0	0	0
mislocalization	0	2	2	0	0	2

Contains *otIs173[*P*rgef-1::dsRed]*, *n*=50

K

hlh-15(tm1824)

Neuron (%)	I3	I4	I6	M1	M4	M5
wild type	100	100	100	100	100	98
missing	0	0	0	0	0	0
mislocalization	0	0	0	0	0	2

Contains *otIs173[*P*rgef-1::dsRed]*, *n*=50

L

hlh-19(tm3105)

Neuron (%)	I3	I4	I6	M1	M4	M5
wild type	100	100	100	100	98	98
missing	0	0	0	0	0	0
mislocalization	0	0	0	0	2	2

Contains *otIs173[*P*rgef-1::dsRed]*, *n*=49

Figure S3. Multiple bHLH proteins are required for neurogenesis of MS neurons. Related to Figure 2. (A) Diagram adopted from [S3] showing the *C. elegans* bHLH proteins known to interact with HLH-2. The bHLH proteins involved in muscle but not neuronal development are shown in orange. (B) Disruption of proneural proteins NGN-1 or CND-1 does not result in I4 misspecification nor does it enhance I4 misspecification in *hlh-2* mutants. (C) Confocal images showing the transformation of the I3 neuron (wild type, arrows and insets) into a non-neuronal cell (arrowheads and insets) and the quantification of I3 neurogenesis defects in *cnd-1* mutants. (D) Confocal images showing the absence of the M1 neuron (wild type, arrows and insets) in *ngn-1* mutants (arrowheads and insets) and the quantification of M1 neurogenesis defects in *ngn-1* mutants. (E-L) The generation of MS-derived neurons is grossly normal in bHLH mutants (E) *lin-32*, (F) *hlh-4*, (G) *hlh-6*, (H) *hlh-10*, (I) *hlh-12*, (J) *hlh-13*, (K) *hlh-15*, and (L) *hlh-19*. Scale bar, 20 μm.

A

Genotype	% I4-to-muscle transformation	*n*	Other defects
wild type[a]	0	100	
let-19(n5470)[a]	14	900	
let-19(n5563)[a]	9	600	
let-19(ok331)[b]	5	55	Unc Egl Pvl
dpy-22(n5571)[a]	8	400	
dpy-22(n5572)[a]	15	300	
dpy-22(n5573)[a]	11	500	
dpy-22(n5574)[a]	10	500	
dpy-22(n5662)[a]	10	400	
dpy-22(e652)	16	43	Dpy Unc Gro Egl
dpy-22(bx92)[c]	12	34	
dpy-22(sy622)[d]	6.5	200	Dpy Unc Gro Egl

a. Contains *oxIs322[*P*myo-2::mCh::H2B]* and *nIs310[*P*nlp-13::gfp]*
b. Homozygous mutant progeny of *let-19 (ok331)/+* mother were scored
c. Contains *pal-1(e2091)* and *him-5(e1490)*
d. Contains *nIs310[*P*nlp-13::gfp]*

B

Genotype[a]	% I4-to-muscle transformation	*n*	Other defects
Vector(RNAi)	0	200	
dpy-22(RNAi)	2	200	
dpy-22(n5572); vector(RNAi)	3	100	
dpy-22(n5572); dpy-22(RNAi)	2	100	
let-19(RNAi)	1	200	
let-19(n5470); vector(RNAi)	6	100	
let-19(n5470); let-19(RNAi)	19	177	Gro Ste Emb

a: Contains *oxIs322[*P*myo-2::mCherry::h2b]* and *nIs310[*P*nlp-13::gfp]*

C

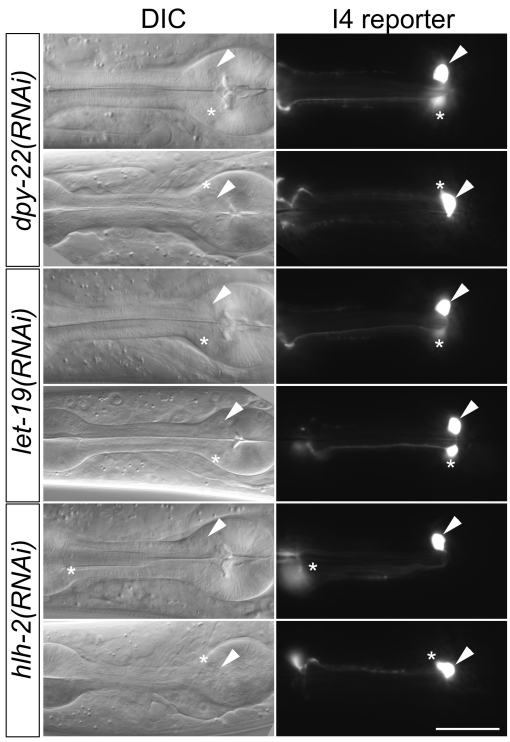

D

Genotype[a]	% I4-to-muscle transformation	*n*
Ex[Pnlp-13::let-19(RNAi)]	0	100
Ex[Pnlp-13::dpy-22(RNAi)]	0	100
Ex[Pnlp-13::hlh-2(RNAi)]	0	100

a: Contain *oxIs322[Pmyo-2::mCherry::H2B]* and *nIs310[Pnlp-13::gfp]*.

Figure S4. Disruption of the Mediator subunits LET-19 and DPY-22 leads to I4 misspecification. Related to Figure 3. (A) The *dpy-22* and *let-19* alleles examined cause incomplete penetrances of I4 misspecification. (B) Further reduction of DPY-22 or LET-19 function by RNAi in *dpy-22* or *let-19* mutants does not significantly enhance I4 misspecification. (C) Cell-specific RNAi by expressing coding fragments of *dpy-22*, *let-19*, or *hlh-2* under the *nlp-13* promoter in late embryos does not disrupt I4 specification. The positions of I4 and M2 are marked by arrowheads and asterisks, respectively. I4 reporter, $P_{nlp\text{-}13}$*::gfp*. (D) Quantification of cell-specific RNAi. Scale bar, 20 μm.

A

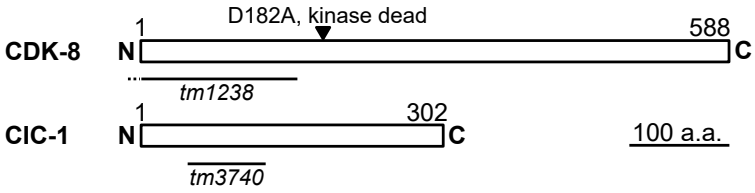

B

Genotype	% I4-to-muscle transformation	*n*	Other defects
wild type[a]	0	100	
dpy-22(n5572)[a]	3	100	
let-19(n5470)[a]	11	100	
hlh-2(bx115)[b]	0	100	
cdk-8(tm1238)[a]	1	100	Dpy
cic-1(tm3740)[a]	1	100	Dpy
cdk-8(tm1238); dpy-22(n5572)[a]	13	300	Dpy Egl
cic-1(tm3740); dpy-22(n5572)[a]	7	100	Dpy Egl
cdk-8(tm1238); let-19(n5470)[a]	N.D.	N.D.	Let
let-19(n5470); cic-1(tm3740)[a]	N.D.	N.D.	Let
hlh-2(bx115) cdk-8(tm1238)[b]	2	200	Dpy
hlh-2(bx115); cic-1(tm3740)[b]	1	300	Dpy

a: Contains *oxIs322[*Pmyo-2::mCherry::h2b*]* and *nIs310[*Pnlp-13::gfp*]*
b: Contains *nIs310[*Pnlp-13::gfp*]*

C

cdk-8(tm1238); cnd-1(gk781)

Neuron (%)	I3	I4	I6	M1	M4	M5
wild type	78	98	100	100	98	100
missing	22	0	0	0	0	0
mislocalization	0	2	0	0	2	0

Contains *otIs173[*Prgef-1::dsRed*]*, *n*=55

D

cdk-8(tm1238); ngn-1(ok2200)

Neuron (%)	I3	I4	I6	M1	M4	M5
wild type	100	87	98	40	100	93
missing	0	0	0	45	0	0
mislocalization	0	13	2	15	0	7

Contains *otIs173[*Prgef-1::dsRed*]*, *n*=60

E

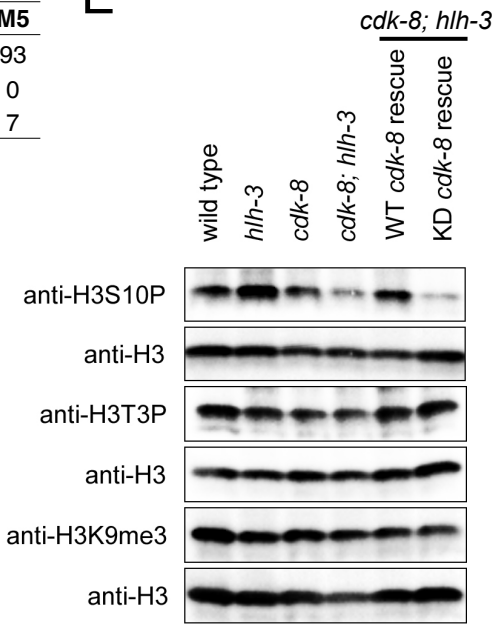

F

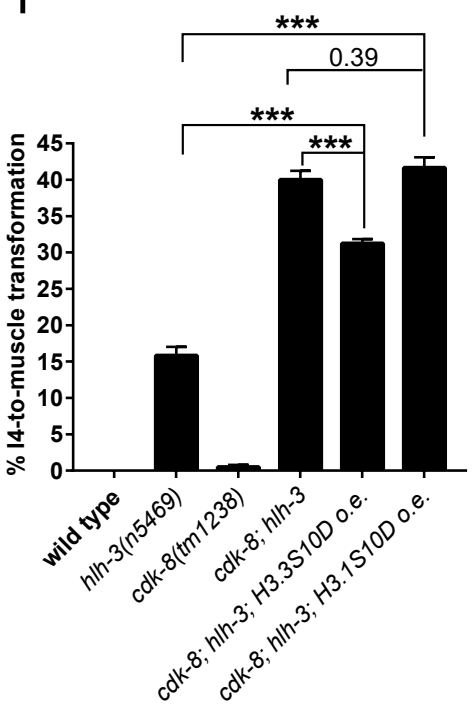

Figure S5. CDK-8 functions together with Mediator and in parallel to HLH-3 to promote I4 neurogenesis. Related to Figure 5. (A) Schematics showing the protein domains of CDK-8 and CIC-1 and the molecular lesions of specified *cdk-8* and *cic-1* alleles. (B) Introducing the *cdk-8* or *cic-1* allele into Mediator or *hlh-2* mutants does not enhance I4 misspecification, suggesting that CDK-8 and CIC-1 function in the same pathway as Mediator and HLH-2 to promote I4 neurogenesis. Dpy, dumpy; Egl, egg-laying defective; Emb, embryonic lethal; Gro, slow growing; Let, lethal; Pvl, protruding vulva; Ste, sterile; Unc, uncoordinated; N.D., not determined. (C) *cdk-8; cnd-1* double mutants have I3 misspecification similar to that of *cnd-1* single mutant (compared to Fig. S3C). (D) *cdk-8; ngn-1* double mutants have M1 misspecification similar to that of *ngn-1* single mutant (compared to Fig. S3D). (E) Western blot showing significantly reduced H3S10 phosphorylation in *cdk-8; hlh-3* double mutants; this reduced phosphorylation is rescued by wild-type (WT) but not kinase-dead (KD) CDK-8 overexpression. H3T3 phosphorylation and H3K9me3 levels remain unaffected. The significant global decrease in H3S10 phosphorylation might be a result of synergistic effects of *cdk-8* and *hlh-3* single mutants, as *hlh-3* mutant animals likely have higher serotonin levels because of the presence of extra serotonergic NSM-like neurons ([S2], Fig. S2I legend), and both serotonin and the CDK8 complex have been implicated in stress responses in metazoa [S4–7]. H3S10 phosphorylation has been shown to be sensitive to stress response [S8,S9] and thus could be more significantly affected in *cdk-8; hlh-3* double mutants. The blot is representative of two biological repeats. (F) Overexpression of a phosphomimetic His3.3 protein HIS-71 but not of His3.1 protein HIS-9 using the native histone promoter partially suppresses I4 misspecification in *cdk-8; hlh-3* double mutants. *n*=100-400 for three independent experiments. Data represent mean ± s.e.m.. ***, P<0.001 by student's t-test.

A

egl-27(ok1670)

Neuron (%)	I3	I4	I6	M1	M4	M5
wild type	100	100	100	100	100	88
missing	0	0	0	0	0	0
mislocalization	0	0	0	0	0	12

n=40

B

sem-4(n1971)

Neuron (%)	I3	I4	I6	M1	M4	M5
wild type	100	100	100	100	100	100
missing	0	0	0	0	0	0
mislocalization	0	0	0	0	0	0

n=40

C

Genotype[a]	% I4-to-muscle transformation	*n*
Vector(RNAi)	0	200
egl-27(RNAi)	0	200
sem-4(RNAi)	0	200
ceh-6(RNAi)	0	200
sox-2(RNAi)_clone1	0	200
sox-2(RNAi)_clone2	0	200
set-2(RNAi)	0	200
set-16(RNAi)	1.5	200
ash-2(RNAi)	0	200
wdr-5.1(RNAi)	0	200
rbbp-5(RNAi)	0	200
jmjd-3.1(RNAi)	0	200
cfp-1(RNAi)	0	200
dpy-30(RNAi)	0	200

a: Contains *oxIs322[Pmyo-2::mCh::H2B]* and *nIs310[Pnlp-13::gfp]*.

D

Genotype[a]	% I4-to-muscle transformation	*n*
hlh-3(n5469); Vector(RNAi)	9	200
hlh-3(n5469); egl-27(RNAi)	10.5	200
hlh-3(n5469); sem-4(RNAi)	11	200
hlh-3(n5469); ceh-6(RNAi)	13.5	200
hlh-3(n5469); sox-2(RNAi)_clone1	14	200
hlh-3(n5469); sox-2(RNAi)_clone2	12	200
hlh-3(n5469); set-2(RNAi)	10	200
hlh-3(n5469); set-16(RNAi)	40	200
hlh-3(n5469); ash-2(RNAi)	8	200
hlh-3(n5469); wdr-5.1(RNAi)	10	200
hlh-3(n5469); rbbp-5(RNAi)	10.5	200
hlh-3(n5469); jmjd-3.1(RNAi)	11	200
hlh-3(n5469); cfp-1(RNAi)	6	200
hlh-3(n5469); dpy-30(RNAi)	15	200

a: Contains *oxIs322[Pmyo-2::mCh::H2B]* and *nIs310[Pnlp-13::gfp]*.

E

lin-12(n137sd)

Neuron (%)	I3	I4	I6	M1	M4	M5
wild type	100	100	100	100	100	98
missing	0	0	0	0	0	0
mislocalization	0	0	0	0	0	2

n=45

F

lin-12(n941)

Neuron (%)	I3	I4	I6	M1	M4	M5
wild type	100	100	92	98	100	92
missing	0	0	0	0	0	0
mislocalization	0	0	8	2	0	8

n=40

G

Genotype[a]	% I4-to-muscle transformation	*n*	Note
wild type	0	200	
lin-12(RNAi)	0	200	
glp-1(RNAi)	0	200	
lag-1(RNAi)	0	30	Emb, Lva
hlh-3(n5469)	14	100	
hlh-3; lin-12(RNAi)	11.5	200	
hlh-3; glp-1(RNAi)	10	200	
hlh-3; lag-1(RNAi)	N/A	N/A	Emb
cdk-8(tm1238); hlh-3(n5469)	42	200	Dpy, Egl
cdk-8; hlh-3; lin-12(RNAi)	37	200	
cdk-8; hlh-3; glp-1(RNAi)	37.5	8	Emb, Ste

a: Contains *oxIs322[Pmyo-2::mCh::H2B]* and *nIs310[Pnlp-13::gfp]*.

Figure S6. Factors required for Y-to-PDA transdifferentiation are dispensable for I4 neurogenesis. Related to Figure 5. (A, B) In the Y-to-PDA (epithelial-to-neuron) mutants (A) *egl-27(ok1670)* and (B) *sem-4(n1971)*, the mesoderm-derived neurons I3, I4, I6, M1, M4, and M5 are generated normally. (C, D) RNAi knockdown of the genes involved in the Y-to-PDA transdifferentiation does not induce or enhance I4 misspecification in (C) wild-type or (D) *hlh-3* mutant animals. By contrast, RNAi of the H3K4 methyltransferase gene *set-16* (which is not involved in Y-to-PDA transdifferentiation) significantly enhances I4 neurogenesis defects in *hlh-3* mutants, suggesting that Y-to-PDA transdifferentiation and I4 neurogenesis depend on distinct molecular pathways. (E, F) Notch signaling required for Y-to-PDA transdifferentiation is likely dispensable for I4 neurogenesis. In the gain- and loss-of-function Notch mutants (E) *lin-12(n137sd)* and (F) *lin-12(n941)*, respectively, the mesoderm-derived neurons I3, I4, I6, M1, M4, and M5 are generated normally. (G) RNAi knockdown of the Notch genes *lin-12*, *glp-1* or *lag-1* does not significantly affect I4 neurogenesis in wild-type, *hlh-3* or *cdk-8; hlh-3* mutant animals. Dpy, dumpy; Egl, egg-laying defective; Emb, embryonic lethal; Lva, larval arrest; Ste, sterile; N/A, not assayed.

Supplemental Experimental Procedures

Strains. All *C. elegans* strains were handled and maintained at 22°C as described previously [S10] unless noted otherwise. We used the Bristol strain N2 as the wild-type strain. The mutations used are listed below:
LGI: *ccIs4251[*P_{myo-3}*::gfp(NLS)::LacZ,* P_{myo-3}*::gfp(mitochondrially targeted), dpy-20(+)], cdk-8(tm1238), hlh-2(bx115, n5287, tm1768ts), sem-4(n1971).*
LGII: *egl-27(ok1670), hlh-3(n5469, n5564, n5566, ot354, tm1688), hlh-6(tm299), let-19(n5470, n5563, ok331), oxIs322[*P_{myo-2}*::mCherry::H2B,* P_{myo-3}*::mCherry::H2B, Cbr-unc-119(+)].*
LGIII: *cic-1(tm3740), cnd-1(gk718, gk781), hlh-4(tm604), jsIs682[*P_{rab-3}*::gfp::rab-3, lin-15(+)], lin-12(n137sd, n941), otIs173[*P_{rgef-1}*::dsRed2,* P_{ttx-3}*::gfp], nIs695[*P_{ceh-22}*::ceh-22::mCherry,* P_{pgp-12}*::mCherry].*
LGIV: *hlh-12(ok1532), ngn-1(ok2200), bcIs25[*P_{tph-1}*::gfp, lin-15(+)], nIs198[*P_{unc-25}*::mStrawberry, lin-15(+)], nIs407[*P_{hlh-2}*::hlh-2::gfp, lin-15(+)], nIs756[*P_{his-9}*::his-9(S10D),* P_{unc-54}*::mCherry].*
LGV: *hlh-10(ok516), kyIs405[*P_{elt-2}*::elt-2::GFP], nIs310[*P_{nlp-13}*::gfp, lin-15(+)], nIs662[*P_{hlh-3}*::hlh-3::gfp,* P_{unc-54}*::mCherry], otIs292[*P_{eat-4}*::eat-4::mCherry, rol-6(su1006)], nIs757[*P_{his-71}*::his-71(S10D),* P_{unc-54}*::mCherry].*
LGX: *dpy-22(bx92, e652, n5571, n5572, n5573, n5574, n5662, sy622), hlh-13(tm2279), hlh-15(tm1824), hlh-19(tm3105), lin-32(e1926), nIs116[*P_{cat-2}*::gfp, lin-15(+)], vsIs48[*P_{unc-17}*::gfp].*
unknown linkage: *nIs324[*P_{tdc-1}*::mStrawberry, lin-15(+)], nIs625[*P_{dpy-22}*::gfp], nIs626[*P_{let-19}*::gfp], nIs656 [*$P_{hsp-16.2}$*::hlh-2(cDNA), rol-6(su1006)], nIs657[*$P_{hsp-16.2}$*::hlh-3(cDNA), rol-6(su1006)], nIs658[*$P_{hsp-16.2}$*::hlh-2(cDNA),* $P_{hsp-16.2}$*::hlh-3(cDNA), rol-6(su1006)], stIs10089[*P_{hlh-1}*::his-24::mCherry, unc-119(+)].*
Extrachromosomal arrays: *nEx2343[*P_{ace-1}*::mCherry], nEx2227[*P_{dpy-22}*::cdk-8(cDNA)::dpy-22 3'-UTR,* P_{unc-54}*::mCherry], nEx2228[*P_{dpy-22}*::cdk-8(cDNA, KD)::dpy-22 3'-UTR,* P_{unc-54}*::mCherry], nEx2554[*P_{dpy-22}*::cyh-1(S5D S327D, cDNA)::dpy-22 3'-UTR,* P_{unc-54}*::mCherry], nEx2555[*P_{dpy-22}*::cyh-1(S5A S327A, cDNA)::dpy-22 3'-UTR,* P_{unc-54}*::mCherry], nEx2557[*P_{dpy-22}*::cdk-7(K34A, cDNA)::dpy-22 3'-UTR,* P_{unc-54}*::mCherry], nEx2558[*P_{dpy-22}*::cdk-7(S157E T163E, cDNA)::dpy-22 3'-UTR,* P_{unc-54}*::mCherry].*

Mutagenesis screen. oxIs322; nIs310 L4 larvae were mutagenized with ethyl methanesulfonate (EMS) as described previously [S10]. About 200,000 F2 or F3 animals were screened non-clonally using a dissecting microscope equipped with UV light. Animals that lacked expression of GFP in the I4 cell, which is stereotypically located in the dorsal side of the posterior bulb of the pharynx in wild-type animals, were picked to single Petri plates. The mutant phenotype was verified by fluorescence and Nomarski DIC imaging using a Zeiss Axioskop2 compound microscope equipped with differential interference contrast (DIC) optics. The I4 cell in mutants was identified based on the position of the I4 nucleus relative to its neighboring pharyngeal cells pm5, pm6, I6 and M1. The presence of an extra muscle-like cell that expressed P_{myo-2}*::mCherry::H2B* also aided the identification of the mutant I4 cell. All of the mutants we described are viable as homozygotes.

Molecular biology and fluorescence reporters. The P_{cat-2}*::gfp,* P_{myo-2}*::mCherry::H2B,* P_{myo-3}*::gfp(NLS)::LacZ,* P_{myo-3}*::gfp(mitochondrially targeted),* P_{rgef-1}*::dsRed2,* P_{unc-17}*::gfp,* P_{tph-1}*::gfp* transcriptional reporters and the P_{eat-4}*::eat-4::mCherry,* P_{elt-2}*::elt-2::gfp,* P_{rab-3}*::gfp::rab-3,* P_{hlh-2}*::hlh-2::gfp* translational reporters have been described previously [S2,S11–19].

The P_{nlp-13}*::gfp* transcriptional reporter was constructed by PCR-amplifying a 2.3 kb *nlp-13* promoter fragment with the oligonucleotides fw-GCGCATGcacctttaaaggcgcacgga and rv-GCCTGCAGCGTTGCATgttggaaccctgga. The resulting product was digested by *Sph*I and *Pst*I and cloned into pPD95.75 (kindly provided by A. Fire) digested by the same restriction enzymes. The plasmid was subsequently injected into the germline of *lin-15(n765)* animals to generate transgenic strains.

The P_{unc-25}*::mStrawberry* transcriptional reporter was made by PCR-amplification using the two primers fw-cgaatttttgcatgcaaaaaacacccactttttgatc and rv-CGGGATCCTCgagcacagcatcactttcgtcagcagc. The resulting PCR product was digested by *Sph*I and *Bam*HI and cloned into pSN199 digested by the same enzymes. pSN199 is a derivative of pPD122.56 (kindly provided by A. Fire) carrying mStrawberry instead of GFP. In short, pSN199 was made by replacing GFP of pPD122.56 with mStraberry from the plasmid mStrawberry 6 (a gift from H. Schwartz). GFP and mStrawberry were swapped using *Age*I and *Eco*RI digestion. The plasmid was subsequently injected into the germline of *lin-15(n765)* animals to generate transgenic strains.

The P_{ceh-22}*::ceh-22::mCherry* and P_{hlh-3}*::hlh-3::gfp* translational reporters were constructed using fosmid recombineering as described [S20]. Briefly, *mCherry* or *egfp* coding sequence was amplified from the plasmid

NM1845 pR6KmCherry (kindly provided by M. Nonet) or NM1835 pR6KGFP [S20], respectively, using the oligonucleotides
fw-GACCTTCAGCAGCTTCTTCCTACATGACCAATACTCAATGGTGGCCTTCTGAATTCATGGTGAGCAAGGGC,
rv-GAGATGTATTCTGGGAAAAATTGACATGGTATAGAGTATTAGAGAAATCAaccggcagatcgtcagtcag ($P_{ceh\text{-}22}$*::ceh-22::mCherry*), and
fw-CATCCACTTCTGGTGATCATCATAGCTTTTATTCGCATACAGAAACTTATagctcaggaggtagcggCA,
rv-CACCCGATTATTTGAGAAAAACAGAAAATATGGTACAACTTAACAGATTAaccggcagatcgtcagtcag ($P_{hlh\text{-}3}$*::hlh-3::gfp*). The PCR products were digested with *Dpn*I to remove template DNA, gel-purified using a QIAquick gel extraction kit (Qiagen), and 1 µl of the purified products were electroporated into L-rhamnose-induced competent bacterial cells that harbored the helper plasmid pREDFlp4 and the fosmid containing full-length *ceh-22* (fosmid 19b10) or *hlh-3* (fosmid 40n18) genomic DNA. Successful recombinants with *mCherry* or *egfp* recombined into the fosmid were selected by kanamycin resistance, with the *kan*^{r} gene subsequently removed by anhydrotetracycline-induced Flp recombination. The correct insertion of *mCherry* or *eGFP* was verified by sequencing. The fosmids were subsequently injected into the germline of wild-type animals to generate transgenic strains.

The $P_{dpy\text{-}22}$*::gfp* transcriptional reporter was generated by overlap extension PCR that fused 2 kb *dpy-22* promoter with the 0.7 kb *egfp* sequence from NM1847 pR6KKanRGFP (kindly provided by M. Nonet), followed by 1 kb *dpy-22* 3'-UTR, using the oligonucleotides fw-ccacagcaaattcaaacatttcttg,
rv-ATGGTGGCGACCGGTGCCATACGTTCGCCGGGCTGCTCGT ($P_{dpy\text{-}22}$),
fw-ACGAGCAGCCCGGCGAACGTATGGCACCGGTCGCCACCAT,
rv-GAAAGAATATAAATATGTAATTGTGACATGAttaTCCGCGGCCGTCCTTGT (*egfp*),
fw-ACAAGGACGGCCGCGGAtaaTCATGTCACAATTACATATTTATATTCTTTC, and
rv-gcaggtggtacacataggaaag (*dpy-22* 3'-UTR). The PCR product was gel-purified using a QIAquick gel extraction kit and subsequently injected into the germline of wild-type animals to generate transgenic strains.

The $P_{let\text{-}19}$*::gfp* transcriptional reporter was generated by overlap extension PCR that fused a 1.8 kb *let-19* promoter with the 0.7 kb *egfp* sequence from NM1847 pR6KKanRGFP, followed by 1.1 kb *let-19* 3'-UTR, using the oligonucleotides fw-cgagaatgaacaaaaggtttcttc,
rv-ATGGTGGCGACCGGTGCCATGTCCTCTGTGGAGTCACGGG ($P_{let\text{-}19}$),
fw-CCCGTGACTCCACAGAGGACATGGCACCGGTCGCCACCAT,
rv-GTACATTTGAAAATTTGATTCACGATATGCttaTCCGCGGCCGTCCTTGT (*egfp*),
fw-ACAAGGACGGCCGCGGAtaaGCATATCGTGAATCAAATTTTCAAATGTAC, and
rv- TGCAGATTCGGACGAAATTGGG (*let-19* 3'-UTR). The PCR product was gel-purified using a QIAquick gel extraction kit and subsequently injected into the germline of wild-type animals to generate transgenic strains.

The $P_{ace\text{-}1}$*::mCherry* transcriptional reporter was generated by overlap extension PCR that fused a 2 kb *ace-1* promoter with the 0.9 kb *mCherry* sequence from pAA64 (kindly provided by K. Oegema), followed by 1.3 kb *unc-54* 3'-UTR from pPD122.56 (kindly provided by A. Fire), using the oligonucleotides fw-ggaagaagaagcagagaagaaa, rv-CTTCTTCACCCTTTGAGACCATGCTTCTTCAACAAATCATAATCGTTTG ($P_{ace\text{-}1}$), fw-GATTATGATTTGTTGAAGAAGCATGGTCTCAAAGGGTGAAGAAG,
rv-CTCAGTTGGAATTcTACGAATGCTACTTATACAATTCATCCATGCC (*mCherry*),
fw-GGCATGGATGAATTGTATAAGTAGCATTCGTAgAATTCCAACTGAG, and
rv-GTCTCATGAGCGGATACATATTTG (*unc-54* 3'-UTR). The PCR product was gel-purified using a QIAquick gel extraction kit and subsequently injected into the germline of wild-type animals to generate transgenic strains.

The $P_{dpy\text{-}22}$*::cdk-8(cDNA, wt* or *KD)::dpy-22 3'-UTR* rescue DNA was generated by overlap extension PCR that fused 2 kb *dpy-22* promoter with the 1.8 kb *cdk-8(wt* or *KD)* cDNA sequence, followed by 2.2 kb *dpy-22* 3'-UTR, using the oligonucleotides fw-ccacagcaaattcaaacatttcttg,
rv-TCATCAATCATTAATGTCATACGTTCGCCGGGCTGCTCGT ($P_{dpy\text{-}22}$),
fw-ACGAGCAGCCCGGCGAACGTATGACATTAATGATTGATGAAAACTTCA,
rv-ATAAATATGTAATTGTGACATGATTATCGATGATATTGTTGTTGCCATTG (*cdk-8*, wt cDNA), or
fw-ACGAGCAGCCCGGCGAACGTATGACATTAATGATTGATGAAAACTTCA,
rv-GATTCTTGAAAATCCCAAAGCAGCAATTTTTACCCT,
fw-AGGGTAAAAATTGCTGCTTTGGGATTTTCAAGAATC,

rv-ATAAATATGTAATTGTGACATGATTATCGATGATATTGTTGTTGCCATTG (*cdk-8*, D182A KD cDNA), and fw-ACAACAATATCATCGATAATCATGTCACAATTACATATTTATATTCTTTC, rv-gatgaggagtgccaaaggataaatg (*dpy-22* 3'-UTR). The PCR products were gel-purified using a QIAquick gel extraction kit and subsequently injected into the germline of wild-type animals to generate transgenic strains.

The 2.4 kb *his-9(S10D)* genomic DNA fragment was generated by PCR-mediated mutagenesis using the oligonucleotides fw-cgctacagcaaacagcaatttaa, rv-TGGAGCCTTTCCTCCGGTGTCTTTACGGGCGGTTTGCTTA (P_{his-9}), fw-TAAGCAAACCGCCCGTAAAGACACCGGAGGAAAGGCTCCA, and rv-caatgttttattctctgataaaaagtcaat (*his-9(S10D)*). The PCR product was gel-purified using a QIAquick gel extraction kit and the point mutation was verified by sequencing. It was subsequently injected into the germline of wild-type animals to generate transgenic strains.

The 3.7 kb *his-71(S10D)* genomic DNA fragment was generated by PCR-mediated mutagenesis using the oligonucleotides fw-gtgttgttccctttcattttagc, rv-AGGAGCTTTTCCTCCAGTGTCTTTACGCGCGGTTTGCTTG (P_{his-71}), fw-CAAGCAAACCGCGCGTAAAGACACTGGAGGAAAAGCTCCT, and rv-cacacagaaatgcttccaacaaa (*his-71(S10D)*). The PCR product was gel-purified using a QIAquick gel extraction kit and the point mutation was verified by sequencing. It was subsequently injected into the germline of wild-type animals to generate transgenic strains.

The P_{dpy-22}*::cyh-1(cDNA, AA)::dpy-22 3'-UTR* rescue DNA was generated by overlap extension PCR that fused 2 kb *dpy-22* promoter with the 1 kb *cyh-1(AA)* cDNA sequence, followed by 2.2 kb *dpy-22* 3'-UTR, using the oligonucleotides fw-ccacagcaaattcaaacatttcttg, rv-TGTGTCGCCGTCGCGTACATACGTTCGCCGGGCTGCTCGT (P_{dpy-22}), fw-ACGAGCAGCCCGGCGAACGTATGTACGCGACGGCGACACACAAAAACG, rv-GAATATAAATATGTAATTGTGACATGATCAATTAATTTCGTCATCCGCATCAACTGGC (*cyh-1AA*), fw-GCGGATGACGAAATTAATTGATCATGTCACAATTACATATTTATATTCTTTC, and rv-gatgaggagtgccaaaggataaatg (*dpy-22* 3'-UTR). The 5.2 kb final PCR product was gel-purified using a QIAquick gel extraction kit and the point mutations were verified by sequencing. It was subsequently injected into the germline of wild-type animals to generate transgenic strains.

The P_{dpy-22}*::cyh-1(cDNA, DD)::dpy-22 3'-UTR* rescue DNA was generated by overlap extension PCR that fused 2 kb *dpy-22* promoter with the 1 kb *cyh-1(DD)* cDNA sequence, followed by 2.2 kb *dpy-22* 3'-UTR, using the oligonucleotides fw-ccacagcaaattcaaacatttcttg, rv-TGTGTGTCCGTCGCGTACATACGTTCGCCGGGCTGCTCGT (P_{dpy-22}), fw-ACGAGCAGCCCGGCGAACGTATGTACGCGACGGACACACAAAAACG, rv-GAATATAAATATGTAATTGTGACATGATCAATTAATTTCGTCATCGTCATCAACTGGC (*cyh-1DD*), fw-GACGATGACGAAATTAATTGATCATGTCACAATTACATATTTATATTCTTTC, and rv-gatgaggagtgccaaaggataaatg (*dpy-22* 3'-UTR). The 5.2 kb final PCR product was gel-purified using a QIAquick gel extraction kit and the point mutations were verified by sequencing. It was subsequently injected into the germline of wild-type animals to generate transgenic strains.

The P_{dpy-22}*::cdk-7(cDNA, KD)::dpy-22 3'-UTR* rescue DNA was generated by overlap extension PCR that fused 2 kb *dpy-22* promoter with the 1.1 kb *cdk-7(KD)* cDNA sequence, followed by 2.2 kb *dpy-22* 3'-UTR, using the oligonucleotides fw-ccacagcaaattcaaacatttcttg, rv-GTATCGTAACGTCTACTCATACGTTCGCCGGGCTGCTCGT (P_{dpy-22}), fw-ACGAGCAGCCCGGCGAACGTATGAGTAGACGTTACGATACAATA, rv-CTCGATCCTAGTTTGATTTTTGCAATAGCCACACATTCGCCCG, fw-CGGGCGAATGTGTGGCTATTGCAAAAATCAAACTAGGATCGAGAGAA, rv-ATAAATATGTAATTGTGACATGATTAATCAAAATTCAATCGTCGAACGG (*cdk-7KD*), fw-GACGATTGAATTTTGATTAATCATGTCACAATTACATATTTATATTCTTTC, and rv-gatgaggagtgccaaaggataaatg (*dpy-22* 3'-UTR). The 5.3 kb final PCR product was gel-purified using a QIAquick gel extraction kit and the point mutation was verified by sequencing. It was subsequently injected into the germline of wild-type animals to generate transgenic strains.

The P_{dpy-22}*::cdk-7(cDNA, EE)::dpy-22 3'-UTR* rescue DNA was generated by overlap extension PCR that fused 2 kb *dpy-22* promoter with the 1.1 kb *cdk-7(EE)* cDNA sequence, followed by 2.2 kb *dpy-22* 3'-UTR, using the

oligonucleotides fw-ccacagcaaattcaaacatttcttg,
rv-GTATCGTAACGTCTACTCATACGTTCGCCGGGCTGCTCGT (P_{dpy-22}),
fw-ACGAGCAGCCCGGCGAACGTATGAGTAGACGTTACGATACAATA,
rv-ACCTGATGCTCGTAATTTCTGTTTGGCTCTCCGAAGAATCGAGCCAAACC,
fw-TTCTTCGGAGAGCCAAACAGAAATTACGAGCATCAGGTTGTGACAAGATGGT,
rv-ATAAATATGTAATTGTGACATGATTAATCAAAATTCAATCGTCGAACGG (*cdk-7EE*),
fw-GACGATTGAATTTTGATTAATCATGTCACAATTACATATTTATATTCTTTC, and
rv-gatgaggagtgccaaaggataaatg (*dpy-22* 3'-UTR). The 5.3 kb final PCR product was gel-purified using a QIAquick gel extraction kit and the point mutations were verified by sequencing. It was subsequently injected into the germline of wild-type animals to generate transgenic strains.

The $P_{hsp-16.2}$*::hlh-2(cDNA)* heat-shock plasmid was constructed by amplifying 1.2 kb *hlh-2* cDNA from reverse transcribed first-strand cDNA synthesized from total wild-type RNA (SuperScript III, Invitrogen) using following oligos:
fw-TTGACAGCGCTAGCATGGCGGATCCAAATAGCCAAC, and
rv-TTGACAGCCCATGGTTAAGCGTAATCTGGTACGTCGTATGGGTAAAACCGTGGATGTCCAAACTGC.
The PCR product was gel purified using a QIAquick gel extraction kit, digested with *Nhe*I, *Nco*I and ligated with the heat-shock vector pPD49.78 (kindly provided by Fire. A). The plasmid was verified by sequencing and was subsequently injected into the germline of wild-type animals to generate transgenic strains.

The $P_{hsp-16.2}$*::hlh-3(cDNA)* heat-shock plasmid was constructed by amplifying 0.5 kb *hlh-3* cDNA from reverse transcribed first-strand cDNA synthesized from total wild-type RNA (SuperScript III, Invitrogen) using following oligos:
fw-TTGACAGCGCTAGCATGACCGCATCCACCTCCTCA, and
rv-
TTGACAGCCCATGGTTAAGCGTAATCTGGTACGTCGTATGGGTAATAAGTTTCTGTATGCGAATAAAA
GCT. The PCR product was gel purified using a QIAquick gel extraction kit, digested with *Nhe*I, *Nco*I and ligated with the heat-shock vector pPD49.78 (kindly provided by Fire. A). The plasmid was verified by sequencing and was subsequently injected into the germline of wild-type animals to generate transgenic strains.

The bacterial strains expressing small interfering RNAs that target the following genes either were not available from the Ahringer [S21] or the ORFeome [S22] RNAi library or contained plasmids with incorrect inserts and were constructed as follows. The genomic DNA fragment spanning both exons and introns for *let-19* was amplified using the oligonucleotides fw-TCGCAAGCTTGTCCTCAACTTCAGCTGGAAAT and
rv-AGAGAAGCTTGGAGTTTCCAGTCCAAGATCTT. The PCR product was gel-purified using a QIAquick gel extraction kit, digested with *Hin*dIII, ligated with *Hin*dIII digested RNAi vector pL4440 [S22], and transformed into HT115 *E. coli* cells. All RNAi clones were verified by sequencing.

The tissue-specific RNAi transgenes P_{nlp-13}*::dpy-22*, P_{nlp-13}*::let-19* and P_{nlp-13}*::hlh-2* were constructed by amplifying 2.2 kb sense and antisense gene fragments as well as 2.3 kb *nlp-13* promoter using following oligos:
fw-ccacctttaaaggcgcacgga,
rv-CGAAGGTTGGTTTTCCGGAGGTTGGAACCctggaagaaagaa (P_{nlp-13}, sense);
fw-ctttcttccagGGTTCCAACCTCCGGAAAACCAACCTTCGA,
rv-CAGCCATTTCAGCATCGTCAG (*dpy-22*, sense);
fw-ccacctttaaaggcgcacgga,
rv-TGACGATGCTGAAATGGCTGGTTGGAACCctggaagaaagaa (P_{nlp-13}, antisense);
fw-ctttcttccagGGTTCCAACCAGCCATTTCAGCATCGTCAG,
rv-CTCCGGAAAACCAACCTTCGA (*dpy-22*, antisense);
fw-ccacctttaaaggcgcacgga,
rv-cagcgcacCTTGGCGGAGGAGTTGGAACCctggaagaaagaa (P_{nlp-13}, sense);
fw-ctttcttccagGGTTCCAACTCCTCCGCCAAGgtgcgct,
rv-GACTCCGAATTTTGTGCCATCT (*let-19*, sense);
fw-ccacctttaaaggcgcacgga,
rv-ATGGCACAAAATTCGGAGTCGTTGGAACCctggaagaaagaa (P_{nlp-13}, antisense);
fw-ctttcttccagGGTTCCAACGACTCCGAATTTTGTGCCATCT,
rv-TCCTCCGCCAAGgtgcgct (*let-19*, antisense);

fw-ccacctttaaaggcgcacgga,
rv-AGTTGGCTATTTGGATCCGCGTTGGAACCctggaagaaagaa (P_{nlp-13}, sense);
fw-ctttcttccagGGTTCCAACGCGGATCCAAATAGCCAACTTA,
rv-CTTTCTCGAGCATTATTCTGTGA (*hlh-2*, sense);
fw-ccacctttaaaggcgcacgga,
rv-CAGAATAATGCTCGAGAAAGGTTGGAACCctggaagaaagaa (P_{nlp-13}, antisense);
fw-ctttcttccagGGTTCCAACCTTTCTCGAGCATTATTCTGTGA,
rv-GCGGATCCAAATAGCCAACTTA (*hlh-2*, antisense).
The P_{nlp-13}*::sense* and P_{nlp-13}*::antisense* fragments were generated using overlap PCR, purified and mixed at a final concentration of 5 ng/μl and injected with 5 ng/μl of P_{unc-54}*::mCherry* and 100 ng/μl of pcDNA3 into the germline of wild-type animals to generate transgenic strains.

RNAi treatments. RNAi experiments were performed by feeding worms with bacteria expressing small interference RNAs, as described previously [S21,S22]. Briefly, HT115 *E. coli* cells carrying RNAi clones were cultured overnight in LB liquid media supplemented with 75 mg/L ampicillin. 30 μl of bacterial culture were seeded into individual wells of 24-well NGM plates supplemented with 1 mM IPTG and 75 mg/L ampicillin, and the plates were incubated at room temperature (22°C) overnight (>12 hrs) to induce siRNA expression. For RNAi experiments, three to ten L2 larvae were transferred to individual wells of the RNAi plates, grown at room temperature (22°C) for three to four days, and the F1 progeny were scored for I4 GFP expression. Worms that lacked GFP expression specifically in I4 were scored as I4-defective. Bacteria expressing the empty RNAi vector pL4440 were used as a control.

Western blots. Worms were grown on 100 mm plates with *E. coli* OP50 bacterial lawn until the *E. coli* was almost depleted; two plates of worms were harvested for each genotype. Worm pellets were flash-frozen in liquid nitrogen, thawed at room temperature, and resuspended in ice-cold 400 μl (final volume) of 1×SDS lysis buffer (2% SDS, 50 mM Tris pH6.8, 10% glycerol). The suspension was sonicated using a Fisher Scientific Sonicator (Model: FB120, 120W, 20 kHz) at 50% output for 3×5 second pulses with 1 min intervals between pulses. Samples were then boiled at 95°C for 20 min. 15 μg of protein was resolved on a 4-15% Bio-Rad Mini-Protean TGX gel, transferred to a nitrocellulose membrane (Whatman Protran, 0.45 μm) and blotted with anti-phospho-H3S10 antibody (Millipore, 06-570) at 1:2000 dilution. The same membrane was stripped and re-blotted with anti-H3 antibody (Santa Cruz, sc-8654r) at 1:1000 dilution. Signals were developed using Chemiluminescence Reagent Plus Kit (PerkinElmer, NEL105), and images were captured with Bio-Rad ChemiDoc MP imaging system. All images were processed using Adobe Photoshop CS4.

Germline transformation. Transgenic lines were constructed using standard germline transformation procedures [S23]. All DNA samples were injected at a final concentration of 10 ng/μl. We used P_{unc-54}*::mCherry* or P_{pgp-12}*::4×NLS::mCherry* as a coinjection marker when needed at 5 ng/μl, and we co-injected pcDNA3 at 100 ng/μl for each injection. For non-integrated transgenic lines that carry extrachromosomal arrays, at least two independent lines were analyzed and averages are shown.

Yeast two-hybrid assay. The yeast two-hybrid assay was performed following the manufacturer's protocol (Clontech). Briefly, fresh Yeast Gold colonies (<1 week old) were cultured in YPD liquid medium at 30°C to the $O.D._{600}$ of 0.5, harvested, washed, and resuspended in 1.1 × TE/LiAc. 100 ng of bait and prey plasmids were mixed with 50 μg of denatured salmon sperm carrier DNA and were transformed into competent yeast cells in the presence of 1× PEG/LiAc. The cell mix was then plated on both –Leu–Trp and –Leu–Trp–His–Ade dropout plates and was allowed to grow at 30°C for 2-3 days. Single colonies that grew on the double and quadruple dropout plates were resuspended in H_2O and respotted to fresh dropout plates, which were grown at 30°C for 2 days. Images of the respotted plates were captured using a Canon Powershot A590 digital camera (Canon) and processed by Photoshop CS4 software (Adobe).

Heat shock. To induce HLH-2 and HLH-3 overexpression, L1 larval transgenic animals carrying the $P_{hsp-16.2}$*:: hlh-2/3* transgene were picked to a fresh plate spotted with OP50 bacteria and heat-shocked at 34°C for 1 hour. The animals were then placed at 22°C overnight before being examined using a confocal microscope.

Supplemental References

S1. Doonan, R., Hatzold, J., Raut, S., Conradt, B., and Alfonso, A. (2008). HLH-3 is a *C. elegans* Achaete/Scute protein required for differentiation of the hermaphrodite-specific motor neurons. Mech. Dev. *125*, 883–893.
S2. Thellmann, M., Hatzold, J., and Conradt, B. (2003). The Snail-like CES-1 protein of *C. elegans* can block the expression of the BH3-only cell-death activator gene *egl-1* by antagonizing the function of bHLH proteins. Development *130*, 4057–4071.
S3. Grove, C. a, De Masi, F., Barrasa, M.I., Newburger, D.E., Alkema, M.J., Bulyk, M.L., and Walhout, A.J.M. (2009). A multiparameter network reveals extensive divergence between *C. elegans* bHLH transcription factors. Cell *138*, 314–27.
S4. Chaouloff, F., Berton, O., and Mormède, P. (1999). Serotonin and stress. Neuropsychopharmacology *21*.
S5. Xie, Y., Moussaif, M., Choi, S., Xu, L., and Sze, J.Y. (2013). RFX transcription factor DAF-19 regulates 5-HT and innate immune responses to pathogenic bacteria in *Caenorhabditis elegans*. PLoS Genet. *9*, e1003324.
S6. Jin, C., Strich, R., and Cooper, K.F. (2014). Slt2p phosphorylation induces cyclin C nuclear-to-cytoplasmic translocation in response to oxidative stress. Mol. Biol. Cell *25*, 1396–1407.
S7. Wang, K., Yan, R., Cooper, K.F., and Strich, R. (2015). Cyclin C mediates stress-induced mitochondrial fission and apoptosis. Mol. Biol. Cell *26*, 1030–43.
S8. Ke, Q., Li, Q., Ellen, T.P., Sun, H., and Costa, M. (2008). Nickel compounds induce phosphorylation of histone H3 at serine 10 by activating JNK-MAPK pathway. Carcinogenesis *29*, 1276–1281.
S9. Dyson, M.H., Thomson, S., Inagaki, M., Goto, H., Arthur, S.J., Nightingale, K., Iborra, F.J., and Mahadevan, L.C. (2005). MAP kinase-mediated phosphorylation of distinct pools of histone H3 at S10 or S28 via mitogen- and stress-activated kinase 1/2. J. Cell Sci. *118*, 2247–2259.
S10. Brenner, S. (1974). The genetics of *Caenorhabditis elegans*. Genetics *77*, 71–94.
S11. Frøkjaer-Jensen, C., Davis, M.W., Hopkins, C.E., Newman, B.J., Thummel, J.M., Olesen, S.-P., Grunnet, M., and Jorgensen, E.M. (2008). Single-copy insertion of transgenes in *Caenorhabditis elegans*. Nat. Genet. *40*, 1375–83.
S12. Bénard, C., Tjoe, N., Boulin, T., Recio, J., and Hobert, O. (2009). The small, secreted immunoglobulin protein ZIG-3 maintains axon position in *Caenorhabditis elegans*. Genetics *183*, 917–27.
S13. Mahoney, T.R., Liu, Q., Itoh, T., Luo, S., Hadwiger, G., Vincent, R., Wang, Z.-W., Fukuda, M., and Nonet, M.L. (2006). Regulation of synaptic transmission by RAB-3 and RAB-27 in *Caenorhabditis elegans*. Mol. Biol. Cell *17*, 2617–2625.
S14. Nakano, S., Ellis, R.E., and Horvitz, H.R. (2010). Otx-dependent expression of proneural bHLH genes establishes a neuronal bilateral asymmetry in *C. elegans*. Development *137*, 4017–27.
S15. Chase, D.L., Pepper, J.S., and Koelle, M.R. (2004). Mechanism of extrasynaptic dopamine signaling in *Caenorhabditis elegans*. Nat. Neurosci. *7*, 1096–1103.
S16. Serrano-Saiz, E., Poole, R.J., Felton, T., Zhang, F., De La Cruz, E.D., and Hobert, O. (2013). Modular control of glutamatergic neuronal identity in *C. elegans* by distinct homeodomain proteins. Cell *155*, 659–673.
S17. Fire, A., Xu, S., Montgomery, M.K., Kostas, S.A., Driver, S.E., and Mello, C.C. (1998). Potent and specific genetic interference by double-stranded RNA in *Caenorhabditis elegans*. Nature *391*, 806–811.
S18. Lints, R., and Emmons, S.W. (1999). Patterning of dopaminergic neurotransmitter identity among *Caenorhabditis elegans* ray sensory neurons by a TGFbeta family signaling pathway and a Hox gene. Development *126*, 5819–5831.
S19. Murray, J.I., Bao, Z., Boyle, T.J., Boeck, M.E., Mericle, B.L., Nicholas, T.J., Zhao, Z., Sandel, M.J., and Waterston, R.H. (2008). Automated analysis of embryonic gene expression with cellular resolution in *C. elegans*. Nat. Methods *5*, 703–709.
S20. Sarov, M., Schneider, S., Pozniakovski, A., Roguev, A., Ernst, S., Zhang, Y., Hyman, a A., and Stewart, a F. (2006). A recombineering pipeline for functional genomics applied to *Caenorhabditis elegans*. Nat. Methods *3*, 839–44.
S21. Kamath, R.S., Fraser, A.G., Dong, Y., Poulin, G., Durbin, R., Gotta, M., Kanapin, A., Bot, N. Le, Moreno, S., Sohrmann, M., *et al.* (2003). Systematic functional analysis of the *Caenorhabditis elegans* genome using RNAi. Nature *421*, 231–7.
S22. Rual, J., Ceron, J., Koreth, J., Hao, T., Nicot, A., Hirozane-kishikawa, T., Vandenhaute, J., Orkin, S.H., Hill, D.E., Heuvel, S. Van Den, *et al.* (2004). Toward improving *Caenorhabditis elegans* phenome mapping with an ORFeome-based RNAi library. Genome Res *14*, 2162–8.
S23. Mello, C., Kramer, J., Stinchcomb, D., and Ambros, V. (1991). Efficient gene transfer in *C.elegans*: extrachromosomal maintenance and integration of transforming sequences. EMBO J. *10*, 3959–3970.